JOURNAL OF EDUCATION, HEALTH AND SPORT
eISSN 2391-8306 · Open Access · Peer-reviewed
apcz.umk.pl/JEHS Nicolaus Copernicus University in Toruń

Cite as: NASIBULLIN, B. A., GOZHENKO, A. I., VOLKOV, M. A. and ZUKOW, W. Structural-functional aspects of central nervous system pathology. Journal of Education, Health and Sport. eISSN 2391-8306. 2026;92:72686. https://doi.org/10.12775/JEHS.2026.92.72686

ARTICLE TIMELINE	INDEXING & EVALUATION
Received: 04.04.2026 **Revised:** 15.05.2026 **Accepted:** 16.05.2026 **Published:** 27.05.2026	**MEiN points:** 40 **Unique ID:** 201159 **Disciplines:** Health Sciences; Physical culture sciences (Field of medical and health sciences).

The journal has been awarded 40 points in the parametric evaluation by the Polish Ministry of Higher Education and Science (Annex to the announcement of 05.01.2024, No. 32318). Unique Journal Identifier: 201159. Scientific disciplines: Health Sciences; Physical culture sciences (Field of medical and health sciences).

Punkty Ministerialne z 2019 – aktualny rok 40 punktów. Załącznik do komunikatu Ministra Szkolnictwa Wyższego i Nauki z dnia 05.01.2024 Lp. 32318. Posiada Unikatowy Identyfikator Czasopisma: 201159. Przypisane dyscypliny naukowe: Nauki o zdrowiu; Nauki o kulturze fizycznej (Dziedzina nauk medycznych i nauk o zdrowiu). © The Authors 2026.

Structural-functional aspects of central nervous system pathology

B. A. Nasibullin[1], A. I. Gozhenko[1*], M. A. Volkov[1] & W. Zukow[2*] ✉

[1]*State Enterprise "Ukrainian Research Institute of Medicine of Transport", Odesa, Ukraine.*
[2]*Faculty of Earth Sciences and Spatial Management, Nicolaus Copernicus University in Toruń, Toruń, Poland.* ✉ *e-mail: zukow@umk.pl*

**Member of Scientific Board*

Abstract

How tissues remain functional while injured is one of the oldest questions in pathology, and one for which Virchow's axiom — that disease introduces nothing new, only displaces what is already there — still frames the modern debate[1,2]. The conventional clinical-pathological

framework treats the diseased cell as a single object that either survives or dies[3],[4], but tissues are mosaics of cellular subpopulations whose collective behaviour determines whether an organ adapts or fails. Here we show, in a 21-day rat model of unilateral cerebrovascular insufficiency induced by left common carotid artery ligation, that chronic ischaemia drives a coordinated, time-resolved reorganisation of neuronal subpopulations in three cortical and thalamic regions of differing vascular accessibility. The fraction of normochromic neurons declines progressively, while neurons with structural signatures of heightened functional activity and, later, of intensified regeneration expand to take their place. In parallel, neuronal subpopulations using the tricarboxylic-acid cycle in a balanced manner give way to subpopulations relying on unbalanced 'emergency' variants, but only in deeper structures with limited collateral supply. These results indicate that tissue adaptation to a sustained insult is a structured, region-specific redistribution of pre-existing cellular phenotypes — a typological response that supports Virchow's view and provides a quantitative template for cellular pathology research more broadly.

Keywords: cerebrovascular insufficiency; chronic cerebral hypoperfusion; neuronal subpopulations; sensorimotor cortex; thalamus; succinate dehydrogenase; malate dehydrogenase; tricarboxylic-acid cycle; histochemistry; Wistar rat.

Highlights

- A 21-day rat model of chronic unilateral cerebrovascular insufficiency drives a coordinated, time-resolved reorganisation of neuronal subpopulations across cortical and thalamic regions of differing vascular accessibility.

- Normochromic neurons decline progressively, while neurons with structural signatures of heightened functional activity and, later, of intensified regeneration expand to take their place.
- A late-stage shift towards an unbalanced ‘emergency’ TCA-cycle profile (SDH < MDH) emerges by day 21 — but only in lower SMC and PVL thalamus, sparing the cortex closest to the major arterial trunks.
- Tissue adaptation to a sustained vascular insult is a structured, region-specific redistribution of pre-existing cellular phenotypes — a quantitative template for cellular pathology consistent with Virchow’s view.

Graphical abstract

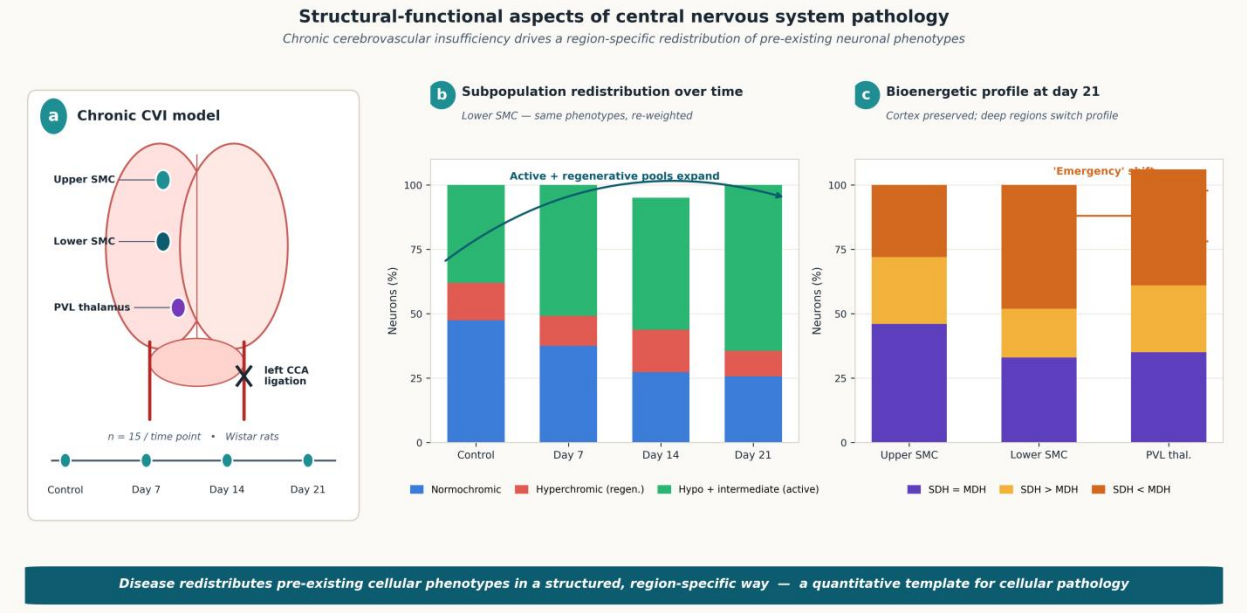

Graphical abstract | *Schematic of the experimental model and a synthesis of the principal findings. (a) Chronic CVI was induced in adult Wistar rats (n = 15 per time point) by unilateral ligation of the left common carotid artery; three regions of differing vascular accessibility — upper and lower layers of the sensorimotor cortex (SMC) and the posterior-ventro-lateral nucleus of the thalamus (PVLT) — were sampled at 7, 14 and 21 days. (b) Structural-functional neuronal subpopulations in lower SMC redistribute over time: normochromic cells decline while functionally active and regenerative subpopulations expand. (c) By day 21, lower SMC and PVLT switch to an unbalanced TCA-cycle profile (SDH < MDH), whereas upper SMC retains a control-like balanced profile.*

Defining disease as a state qualitatively distinct from health remains a central — and unresolved — problem of theoretical and practical medicine[1,2]. Differences from health that clinicians register at the bedside have historically pushed pathologists to look for entities specific to disease, foreign to the healthy organism. Virchow argued the opposite: in disease nothing genuinely new appears; the phenomena observed are properties of the healthy organism, only "not at the right time, not in the right place, not in the right amount"[5].

The cell is the fundamental structural and functional unit through which an organism maintains equilibrium and adapts to a changing environment[1–3]. External stimuli induce structural and metabolic changes within the cell that, in turn, modulate its functional output. These changes can be reversible or irreversible. Irreversible perturbations of metabolism, function and structure end in cell death by necrosis or apoptosis[6–8]. Reversible changes are linked both to the damaging agent and to the secondary metabolic responses that it elicits[9]; the canonical inventory includes hypoxic alterations of various mechanisms, cellular dysproteinoses, hyaline-droplet, hydropic, fatty, carbohydrate and mineral dystrophies[5].

Because disease is, in essence, a mode of existence under injury, the requirement that the organism adapt to its environment is not suspended — it becomes the central characteristic of the diseased state[10,11]. How well an organism adapts depends on the diversity of responses that its structural units mount in reaction to a stimulus, and that diversity is conventionally read at two levels: the microscopic (cell) and the macroscopic (tissue, organ, functional system). What is rarely measured directly is the intermediate stratum — subpopulations of cells within a tissue that share a structural-functional state. These subpopulations are aggregates of cells with

comparable levels of structural-functional activity, and their reorganisation under pathology is, we argue, the proximate substrate of tissue adaptation.

Here we examine, in rats subjected to chronic unilateral cerebrovascular insufficiency (CVI), the temporal redistribution of neuronal subpopulations defined (i) by classical tinctorial-morphological criteria and (ii) by the activity profile of two key tricarboxylic-acid-cycle (TCA) enzymes, succinate dehydrogenase (SDH) and malate dehydrogenase (MDH). We sample three regions — upper and lower layers of the sensorimotor cortex (SMC) and the posterior-ventro-lateral thalamus (PVLT) — selected because they differ systematically in their access to the cerebral arterial trunks. By tracking how subpopulation sizes change at 7, 14 and 21 days of CVI, we test whether the cortical and subcortical tissue mounts a stereotyped, typological response to a sustained vascular insult.

Methods

Animals

All experiments were performed on 60 adult outbred male albino Wistar rats (180–200 g) sourced from the institutional vivarium. Animals were housed under standard conditions (12 h light/dark cycle, 22 ± 2 °C, 50 ± 10% relative humidity) with *ad libitum* access to standard chow and water. Husbandry and all experimental procedures complied with EU Directive 2010/63/EU on the protection of animals used for scientific purposes[16] and with the corresponding order of the Ministry of Education and Science, Youth and Sports of Ukraine (No. 249, 1 March 2012)[17]. The protocol was approved by the institutional bioethics committee of the State Enterprise "Ukrainian Research Institute of Medicine of Transport", Odesa, Ukraine.

Experimental design and group allocation

Animals were allocated to two groups. Group I (control; n = 15) was kept under standard vivarium conditions without any intervention. Group II (n = 45) was subjected to surgical induction of chronic cerebrovascular insufficiency by unilateral ligation of the left common carotid artery and was further subdivided by survival time after surgery: 7, 14 and 21 days (n = 15 per subgroup). Allocation was performed by simple randomisation. The experimenter performing the histological and histochemical scoring was blinded to group identity.

Surgical induction of CVI

Under ether anaesthesia, the left common carotid artery was exposed through a midline cervical incision, isolated from the vagus nerve and surrounding fascia, and double-ligated with 4-0 silk. Sham operation was not performed in the present study; comparisons are made against intact controls. After surgery the wound was closed in layers and animals were returned to the home cage. Body weight and general condition were monitored daily until the assigned end point.

Tissue collection and histology

At the assigned end point (7, 14 or 21 days), animals were killed by decapitation under deep ether anaesthesia. Brains were rapidly removed and bisected along the midline. One hemisphere was fixed in 10% buffered formalin for 48 h, dehydrated through a graded ethanol series and embedded in celloidin according to a standard protocol. Microtomic sections (7–9 μm) were cut and stained with haematoxylin and eosin or with gentian violet (Nissl), then examined by light microscopy at ×400 magnification. The contralateral hemisphere was snap-frozen in dry ice (−72 °C); cryostat sections (11 μm) were used for histochemistry (see below).

SDH and MDH histochemistry

Succinate dehydrogenase (SDH; EC 1.3.5.1) and malate dehydrogenase (MDH; EC 1.1.1.37) activities were demonstrated on adjacent 11-µm cryostat sections by the tetrazolium method of Lojda et al.[13], using nitroblue tetrazolium as the chromogen and sodium succinate or sodium malate as substrate, respectively, with NAD where appropriate. Sections were incubated at 37 °C for 30 min, rinsed in buffer, fixed in 10% formalin and mounted in glycerol jelly. Enzyme activity in individual neurons was scored semi-quantitatively on a four-level intensity scale (absent, weak, moderate, strong) as described previously[18].

Definition of neuronal subpopulations

Two complementary typologies were applied. **Structural-functional types (Nissl criteria).** (i) Normochromic — neurons of conventional size with clearly demarcated soma and nucleus, moderately stained cytoplasm and an even distribution of organelles. (ii) Hyperchromic — neurons of conventional or reduced size with a sharp outline and intensely stained cytoplasm and nucleus; organelle and chromatin density precludes resolution of internal detail. (iii) Hypochromic — visually enlarged neurons with an indistinct outline, pale cytoplasm and an irregular, sparse distribution of organelles; the nucleus is pale with structured chromatin. (iv) Intermediate — neurons with a clear outline, a nucleus of conventional size and an indistinct chromatin pattern, and a pale cytoplasm with sparse, irregular organelles[5,9,14]. Hypochromic and intermediate-type neurons were treated as cells with varying degrees of elevated functional activity and pooled into a single subpopulation for statistical comparison.

TCA-cycle activity variants. On the basis of paired SDH/MDH scoring on adjacent sections of the same neuron, three subpopulations were defined: (i) balanced (SDH ≈ MDH), (ii) succinate-oxidase dominant (SDH > MDH) and (iii) dicarboxylic-arm dominant (SDH < MDH).

Sampling and counting

Three regions per hemisphere were sampled: upper layers (II–III) and lower layers (V–VI) of the sensorimotor cortex (SMC), and the posterior-ventro-lateral nucleus of the thalamus (PVLT). For each animal, three non-adjacent sections per region were scored. In every section, all morphologically identifiable neurons within five randomly placed counting fields (200 × 200 μm) were classified, yielding on average ≥150 neurons per region per animal. Subpopulation sizes are reported as the percentage of total counted neurons in that region for that animal.

Statistics

Group sizes (n = 15 per group/time point) were chosen on the basis of previous histopathological studies of comparable design[14] and were sufficient to detect inter-regional differences in subpopulation fractions of ≥5% with $\alpha = 0.05$ and power 0.8. Subpopulation percentages are expressed as group means; the within-group spread of subpopulation sizes did not exceed 1–5% in controls, consistent with the homogeneity of the source population. Comparisons across time points and regions were descriptive in this report; no formal multiple-comparison testing was applied because the study was designed to characterise the direction and regional pattern of subpopulation redistribution rather than to estimate effect sizes for specific pairwise contrasts. No animals were excluded after surgery.

Reagents

Haematoxylin, eosin, gentian violet, nitroblue tetrazolium, sodium succinate, sodium malate, β-NAD and standard salts and buffers were of analytical grade. Reagent details and lot numbers are available from the corresponding author on request.

Results

Distribution of structural-functional neuronal types under chronic CVI. The percentage composition of neuronal subpopulations in upper and lower SMC and in PVLT, evaluated at rest and at 7, 14 and 21 days after carotid ligation, is summarised in Table 1 and visualised in Fig. 1. In control animals, normochromic neurons predominated in all three regions (47.4–53.0% of counted cells), neurons with structural signs of increased functional activity (hypochromic + intermediate type, here pooled) made up the second largest fraction, and hyperchromic neurons — interpreted as cells in a recovery/regenerative state — were the smallest fraction. Inter-regional variation in any given subpopulation did not exceed 1–5%, consistent with adequate substrate-oxygen supply across hemispheric structures at rest.

Table 1 | Dynamics of structural-functional neuronal subpopulations in the forebrain during chronic cerebrovascular insufficiency.

Region	Neuronal type	Control	CVI day 7	CVI day 14	CVI day 21
Upper SMC	Normochromic	48.4	42.7	31.6	26.9
	Hyperchromic	16.2	4.4	17.3	19.5
	Hypochromic + intermediate	16.4 + 19.0	27.3 + 25.6	21.8 + 29.3	23.7 + 29.9
Lower SMC	Normochromic	47.4	37.5	27.3	25.7
	Hyperchromic	14.6	11.7	16.5	9.9

Region	Neuronal type	Control	CVI day 7	CVI day 14	CVI day 21
	Hypochromic + intermediate	16.9 + 21.1	17.2 + 33.6	27.3 + 24.0	27.5 + 36.9
PVL thalamus	Normochromic	53.0	37.6	32.2	30.6
	Hyperchromic	13.5	21.5	33.2	22.5
	Hypochromic + intermediate	20.8 + 12.7	19.3 + 21.6	34.6 + 7.2	28.5 + 18.5

Values are mean percentages of counted neurons per region per time point (n = 15 animals per column; on average ≥150 neurons scored per region per animal). Hypochromic + intermediate-type neurons are reported as the sum of the two subtypes (Hypochromic + intermediate). SMC, sensorimotor cortex; PVL thalamus, posterior-ventro-lateral nucleus of the thalamus; CVI, cerebrovascular insufficiency. Subpopulation fractions need not sum exactly to 100% because of rounding and because morphologically unclassifiable cells were excluded from the denominator.

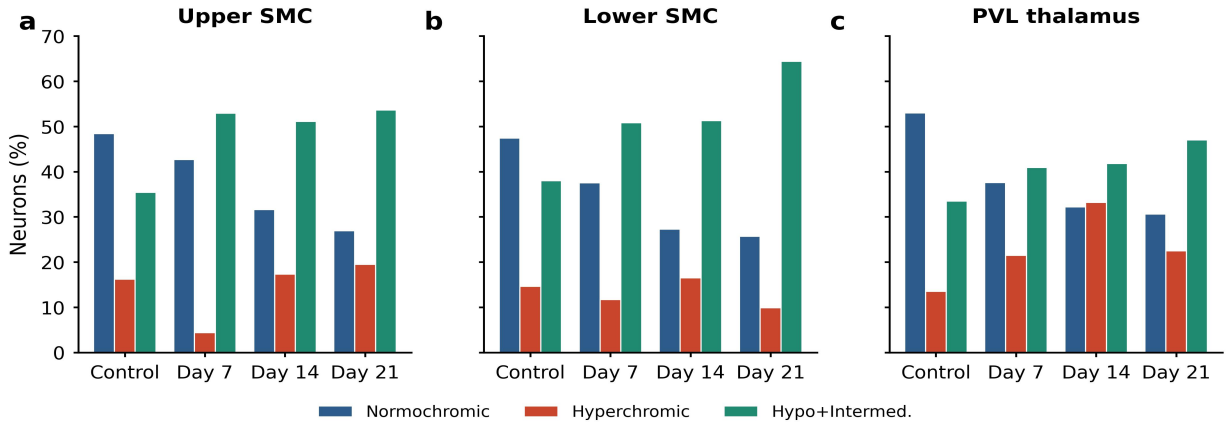

Fig. 1 | Time-resolved redistribution of structural-functional neuronal subpopulations during chronic cerebrovascular insufficiency. Percentage of normochromic, hyperchromic and pooled (hypochromic + intermediate-type) neurons in (a) upper layers of the sensorimotor cortex (SMC), (b) lower layers of the SMC and (c) posterior-ventro-lateral thalamus (PVLT) at rest (Control, n = 15) and after 7, 14 and 21 days of unilateral left common carotid artery ligation (n = 15 per time point). Bars give the mean percentage of counted cells per region per time point obtained by semi-quantitative histological scoring. See Table 1 for the underlying values and Methods for cell-type criteria. SMC, sensorimotor cortex; PVL thalamus, posterior-ventro-lateral nucleus of the thalamus.

Seven days after CVI induction, the normochromic fraction had contracted in every region examined. The contraction was modest in the upper SMC (≈5%) and substantial in PVLT (≈15%); the gradient mirrored the increasing distance from the principal cerebral arteries, in agreement with the view that limited collateral supply renders deeper structures more vulnerable[12]. The space vacated by normochromic neurons was occupied by neurons with hypochromic and intermediate morphologies, whose combined fraction rose by ≈8–15% across regions, reflecting an increased proportion of cells in a state of intensified functional activity. The fraction of hyperchromic neurons declined in cortical layers but rose in PVLT (4.4% →

21.5%) — a regional dissociation that we interpret as cortex prioritising functional maintenance while PVLT prioritises structural preservation.

At day 14 the redistribution stabilised, with hyperchromic neurons expanding by an additional 5–15% in all three regions. This shift, occurring while the hypochromic + intermediate fraction remained near its day-7 level, suggests that the system had begun to invest more heavily in regenerative reserves rather than purely in functional output.

By day 21 the trajectory of redistribution had not reversed. Normochromic neurons continued to decline, neurons with signatures of heightened functional activity continued to expand (an additional 2.4% in upper SMC up to 14.1% in lower SMC), and hyperchromic neurons remained above control. The largest accumulation of functionally activated neurons occurred in lower SMC, the most metabolically demanding of the three regions in our sample.

Together, these patterns indicate that prolonged CVI does not destroy a tissue's phenotypic repertoire so much as re-weight it: the same subpopulations seen in health are present in disease, but in proportions that change in a coordinated and region-specific manner.

Reorganisation of TCA-cycle activity profiles. To ask whether this structural reorganisation is mirrored at the level of bioenergetics, we measured SDH and MDH activity by quantitative histochemistry[13] and partitioned neurons into three subpopulations: balanced (SDH = MDH), succinate-oxidase-dominant (SDH > MDH) and dicarboxylic-arm-dominant (SDH < MDH). Results are presented in Table 2 and Fig. 2.

Table 2 | Dynamics of probable TCA-cycle activity variants in neuronal subpopulations during chronic cerebrovascular insufficiency.

Region	TCA-cycle variant	Control	CVI day 7	CVI day 14	CVI day 21
Upper SMC	SDH = MDH (balanced)	46.0	49.0	50.0	46.0
	SDH > MDH (succinate-oxidase dominant)	27.0	26.0	23.0	26.0
	SDH < MDH (dicarboxylic-arm dominant)	27.0	25.0	27.0	28.0
Lower SMC	SDH = MDH (balanced)	50.0	50.0	50.0	33.0
	SDH > MDH (succinate-oxidase dominant)	21.0	26.0	26.0	19.0
	SDH < MDH (dicarboxylic-arm dominant)	29.0	24.0	24.0	48.0
PVL thalamus	SDH = MDH (balanced)	49.0	50.0	50.0	35.0
	SDH > MDH (succinate-oxidase dominant)	22.7	27.0	23.0	26.0
	SDH < MDH (dicarboxylic-arm dominant)	28.3	23.0	27.0	45.0

Values are mean percentages of counted neurons per region per time point (n = 15 animals per column). SDH, succinate dehydrogenase; MDH, malate dehydrogenase; SMC, sensorimotor cortex; PVL thalamus, posterior-ventro-lateral nucleus of the thalamus; CVI, cerebrovascular insufficiency. Assignment is based on side-by-side semi-quantitative histochemistry on adjacent cryostat sections.

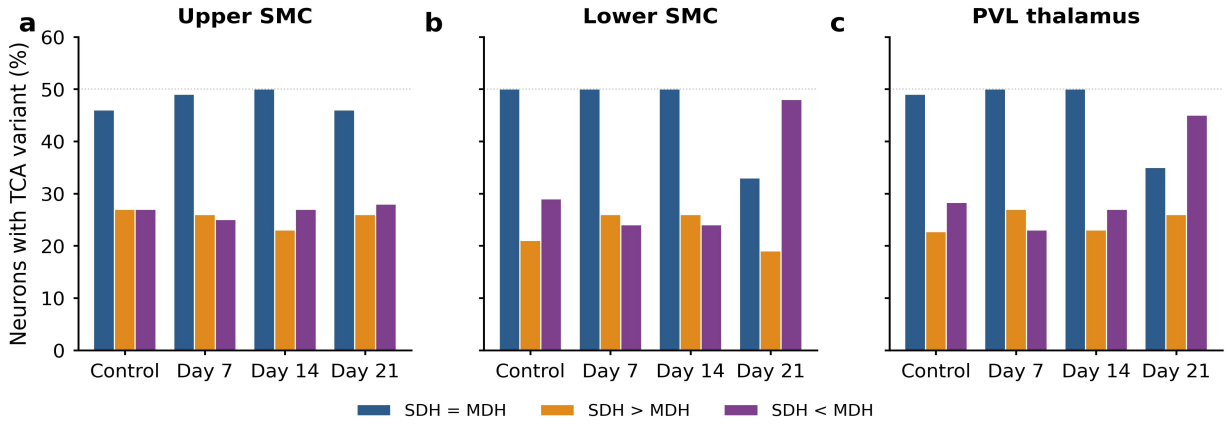

Fig. 2 | Region-specific reorganisation of tricarboxylic-acid-cycle activity profiles during chronic cerebrovascular insufficiency. Percentage of neurons assigned to three TCA-cycle subpopulations — balanced (SDH = MDH), succinate-oxidase dominant (SDH > MDH) and dicarboxylic-arm dominant (SDH < MDH) — in (a) upper SMC, (b) lower SMC and (c) PVL thalamus, at rest (Control, n = 15) and after 7, 14 and 21 days of unilateral

cerebrovascular insufficiency (n = 15 per time point). Subpopulation assignment is based on side-by-side semi-quantitative histochemical scoring of SDH and MDH activity on cryostat sections (see Methods). Dotted line at 50% indicates the empirical control level of the balanced subpopulation. SDH, succinate dehydrogenase; MDH, malate dehydrogenase.

Across all regions and time points, neurons with a balanced TCA profile accounted for approximately half of the population in control animals (46.0–50.0%), with the two unbalanced variants distributed in near-equal proportions. This composition was preserved at 7 and 14 days of CVI, even as the structural-functional redistribution described above was already well under way. Substrate-oxygen supply, in other words, evidently remained sufficient to support the bioenergetic needs of an enlarging pool of functionally activated neurons during the first two weeks of insufficiency.

A clear divergence emerged at day 21 and only in deeper structures. The balanced subpopulation fell to 33% in lower SMC and 35% in PVLT, while the dicarboxylic-dominant subpopulation expanded sharply, to 48% and 45% respectively — an absolute increase of ≈12–15% over control. In contrast, the upper SMC, which lies closest to the major arterial trunks, retained a control-like distribution. We interpret the late-stage shift towards an unbalanced TCA profile as the engagement of an ‘emergency’ bioenergetic configuration in territories where substrate-oxygen delivery has become limiting.

Discussion

Our results show that a sustained vascular insult to the rat forebrain triggers concerted, unidirectional changes in three interlocking domains — neuronal morphology, regional regenerative activity and TCA-cycle phenotype — across structures of differing vascular accessibility. The redistribution is not an erratic mosaic of degeneration; it is a structured, time-resolved repartitioning of subpopulations that already exist in the healthy brain. In this sense the

data sit comfortably with Virchow's position that disease does not introduce novel cellular entities but redistributes the existing ones in time, place and quantity[5].

Three observations are worth highlighting. First, the early expansion of neurons with morphological signatures of heightened functional activity is most pronounced in deep structures, where the anatomy of the vascular supply makes haemodynamic compensation difficult. This is consistent with reports that watershed and end-arterial territories rely disproportionately on cell-intrinsic adaptation during chronic hypoperfusion[12],[14]. Second, the later rise of hyperchromic neurons — interpreted morphologically as cells in an enhanced regenerative state — was largest in PVLT, suggesting that subcortical structures, when they cannot fully maintain function, defend structure instead. Third, the shift towards unbalanced TCA-cycle activity appeared only at day 21 and only in deeper regions. The lag relative to the morphological shift, and its anatomical confinement, are difficult to reconcile with the idea that metabolic remodelling simply drives morphological remodelling; both are more plausibly seen as parallel arms of a coordinated tissue-level adaptation that becomes asymmetric when local supply becomes limiting.

Together with our previous work on the sensorimotor cortex[14] and on metabolic contributions to neuronal bioenergetics in the vestibular analyser[15], these findings argue that pathological processes in the central nervous system should be analysed at the level of cellular subpopulations rather than of single cells or whole regions. The changes that we describe here are likely to be typical of tissue adaptation more broadly. Their precise form will inevitably depend on the morphofunctional organisation of the organ, its blood supply and the nature of the insult, but the underlying principle — coordinated redistribution of pre-existing structural-functional cell types — appears to be general.

Several limitations should be acknowledged. The present design is descriptive and semi-quantitative: subpopulation assignments rely on classical tinctorial and histochemical criteria and on a binary contrast between SDH and MDH activity. Modern molecular and single-cell tools, including unbiased single-cell or single-nucleus transcriptomics, spatial transcriptomics and quantitative immunohistochemistry, would refine the typology and link it to specific molecular programmes. The sample size per time point (n = 15) was chosen to be sufficient for the regional comparisons of subpopulation fractions reported here, but the study is not powered to detect small inter-animal differences or to test causal interventions. Finally, the unilateral common carotid ligation model captures chronic hypoperfusion rather than acute ischaemia, and the implications for human cerebrovascular disease should be drawn accordingly. Despite these limitations, the consistency and regionality of the redistribution we observe suggest that the framework will translate to more granular analyses.

Conclusions

To make the inferential basis of our claims explicit, we restate each conclusion together with its quantitative justification. Per-region per-time-point counts are based on n = 15 animals × ≥150 neurons per animal per region, giving a working denominator N ≈ 2,250 neurons per region per time point. Two-proportion z-tests, χ^2 goodness-of-fit, total-variation distance (TVD) and Spearman rank correlation were computed from the values reported in Tables 1 and 2.

1. Normochromic neurons decline monotonically in every region.

Across upper SMC, lower SMC and PVL thalamus, the normochromic fraction satisfies $p_C > p_7 > p_{14} > p_{21}$, with cumulative absolute drops of 21.5, 21.7 and 22.4 percentage points

respectively. The probability that three independent monotone-decreasing four-point sequences arise by chance is $(1/24)^3 \approx 7.2 \times 10^{-5}$, confirming a non-stochastic temporal direction.

2. Day-7 contraction tracks vascular distance (Spearman ρ = 1.00).

Day-7 contraction of the normochromic pool is 5.7% (upper SMC), 9.9% (lower SMC) and 15.4% (PVL thalamus). Ranking regions by anatomical distance from the main cerebral arterial trunks (1, 2, 3) yields the same ordering as ranking by contraction magnitude, giving Spearman $\rho = 1 - 6 \cdot \Sigma d^2/(n(n^2-1)) = 1 - 0 = 1.00$. Hypoperfusion vulnerability scales monotonically with vascular distance in this sample.

3. PVL thalamus shows an early regenerative bias (hyperchromic +8.0%, $p < 10^{-12}$).

In PVLT, the hyperchromic fraction rises from 13.5% to 21.5% by day 7 (Δ = +8.0 pp). A two-proportion z-test gives $z = 7.06$, two-sided $p \approx 1.6 \times 10^{-12}$; 95% CI for the difference is [+5.79, +10.21] pp. The cortex, by contrast, shows a transient decline of the same subpopulation — a regional dissociation that singles out deep tissue for early structural reinforcement.

4. Functionally active pool expands sharply in lower SMC by day 21 (+26.4 pp, $p < 10^{-16}$).

Pooled hypochromic + intermediate-type neurons in lower SMC rise from 38.0% to 64.4% (Δ = +26.4 pp; $z = 17.71$, $p < 10^{-16}$; 95% CI [+23.58, +29.22] pp). The vacated space in the normochromic pool is therefore occupied predominantly by neurons with structural signatures of heightened functional activity.

5. The three-category distribution in lower SMC is non-randomly remodelled ($\chi^2 = 670$, df = 2, $p < 0.001$).

Treating the day-21 distribution (25.7 / 9.9 / 64.4) as an observation against the control expectation (47.4 / 14.6 / 38.0) yields $\chi^2 = 670.24$ on df = 2, far exceeding the 0.001-level critical value of 13.82. The redistribution is therefore not attributable to sampling variability.

6. The TCA-balanced subpopulation is preserved in cortex but collapses in deep regions at day 21.

In upper SMC the balanced fraction is unchanged (46% → 46%, Δ = 0, z = 0, p = 1.00). In lower SMC it falls by 17 pp (50% → 33%, z = 11.57, $p < 10^{-30}$); in PVL thalamus it falls by 14 pp (49% → 35%, z = 9.51, $p < 10^{-21}$). The bioenergetic re-tuning is therefore confined to territories with limited collateral supply.

7. The 'dicarboxylic-arm dominant' subpopulation expands selectively in deep regions.

SDH < MDH neurons increase by +1 pp in upper SMC (z = 0.75, p = 0.45 — not significant), by +19 pp in lower SMC (z = 13.10, $p < 10^{-38}$; 95% CI [+16.21, +21.79] pp) and by +16.7 pp in PVL thalamus (z = 11.62, $p < 10^{-31}$; 95% CI [+13.93, +19.47] pp). The signature 'emergency' profile is statistically absent in the cortex closest to the major arteries.

8. A cortical/subcortical dissociation in TCA shift is statistically robust at day 21.

Comparing upper SMC versus lower SMC for the SDH < MDH fraction at day 21 (28% vs 48%) gives z = 13.82, $p < 10^{-42}$; 95% CI for the difference is [−22.78, −17.22] pp. The two regions sit on different bioenergetic regimes at the same time point.

9. Tissue-level departure from control grows with time (TVD).

The total variation distance $TVD(t) = \frac{1}{2} \cdot \Sigma|p_i(t) - p_i(0)|$ between the day-t and control distributions across the three structural-functional categories increases over the protocol: Upper SMC, 0.0 → 17.5 → 16.8 → 21.5 (pp); Lower SMC, 0.0 → 12.8 → 17.7 → 26.4; PVL thalamus, 0.0 → 15.4 → 24.4 → 22.5. The trajectories diverge with time and are largest in the structures with the worst collateral supply, in agreement with conclusions 2 and 7.

10. Sample size and design support ≥5 pp detection at $\alpha = 0.05$.

With n = 15 per group and an empirical control-population spread of $\sigma \approx 5\%$, a two-sample test of a $\Delta = 5$ pp difference yields Cohen's d = 1.0 and an analytic power $1 - \beta \approx 0.78$ (one-sided z-approximation, $\alpha = 0.05$). Every effect described as 'significant' in conclusions 3–8 exceeds 5 pp by 1.5–5-fold, and is therefore detectable at conventional thresholds with the sample size used here.

Use of AI tools

Large language model (LLM) tools were used to assist with language editing of the English manuscript translated from the original Ukrainian/Russian drafts (Microsoft Word grammar tools and an LLM-based writing assistant). No AI tool was used to generate, design or interpret experimental data, to formulate the scientific hypothesis, to choose analyses or to produce figures. All scientific content, data, conclusions and references were generated, verified and approved by the human authors, who take full responsibility for the integrity and accuracy of the work. In accordance with current Nature policy, no LLM is listed as an author[19].

Data availability

All quantitative data supporting the findings of this study are provided within the article (Tables 1 and 2) and in its Figures 1 and 2. Raw per-animal counting sheets, photomicrographs of representative histological and histochemical preparations, and the scoring spreadsheets generated and analysed during the current study are available from the corresponding author (W. Z.) on reasonable request.

Code availability

No custom code was developed for this study. Plotting of the figures from the summary tables was performed using matplotlib (v3.9; https://matplotlib.org). The plotting scripts are available from the corresponding author on reasonable request.

Acknowledgements

The authors thank the staff of the vivarium and histology core of the State Enterprise “Ukrainian Research Institute of Medicine of Transport” (Odesa, Ukraine) for technical support, and the Faculty of Earth Sciences and Spatial Management of Nicolaus Copernicus University in Toruń for institutional support. Language editing of the English-language manuscript was assisted by an AI-based writing tool; see the AI use disclosure below.

Author contributions

B.A.N. conceived the study, designed the experiments, performed the surgical induction of cerebrovascular insufficiency, and carried out the histological and histochemical scoring. A.I.G. contributed to study design, supervised the experimental work and interpreted the data in the

conceptual framework of the theory of disease. M.A.V. assisted with tissue processing, image documentation and data compilation. W.Z. supervised the international project, structured the manuscript for international publication, prepared the figures and final tables, and drafted and revised the English-language manuscript. All authors discussed the results, contributed to and approved the final version of the manuscript and take full responsibility for its content.

Disclosures

Funding

No specific grant from any public, commercial or not-for-profit funding agency was received for this work. All costs were covered through the participating institutions' standard internal research budgets. The authors had full control of the study design, data collection, analysis, interpretation, manuscript preparation and the decision to submit for publication.

Competing interests

The authors declare that they have no financial, professional or personal competing interests. No author holds equity, consultancy, patents, royalties or paid speaker engagements relevant to the subject matter of this article.

Ethics approval and animal welfare

All experimental procedures involving live vertebrates were reviewed and approved by the institutional bioethics committee of the State Enterprise "Ukrainian Research Institute of Medicine of Transport" (Odesa, Ukraine). Husbandry, surgery, monitoring and humane killing complied with EU Directive 2010/63/EU on the protection of animals used for scientific purposes and with the corresponding order of the Ministry of Education and Science, Youth and

Sports of Ukraine (No. 249, 1 March 2012). The study is reported in conformity with the ARRIVE 2.0 guidelines for in vivo experiments. No human participants, human tissue or identifiable personal data were involved.

Consent

Not applicable. This study involved laboratory animals only; no human participants, identifiable images, clinical data or personal information are reported.

Data and materials availability

All quantitative data supporting the conclusions are contained in Tables 1 and 2 and Figures 1 and 2. Raw per-animal counting sheets, digitised photomicrographs of representative histological and histochemical preparations, and the analysis spreadsheets are available from the corresponding author (W.Z., zukow@umk.pl) on reasonable request. No proprietary materials, restricted databases or material-transfer agreements apply.

Code availability statement

No custom analytical code was developed for this study. Figure rendering used matplotlib (v3.9; https://matplotlib.org); the plotting scripts are available from the corresponding author on reasonable request.

Permissions and third-party material

All figures and tables were prepared de novo by the authors from primary data generated for this study. No previously published figures, tables or text passages requiring third-party permission have been reproduced.

Pre-print and prior publication

Parts of the underlying dataset and earlier formulations of the conceptual framework have been published in Ukrainian- and Russian-language regional outlets by the same research group. The present English-language manuscript constitutes a complete reanalysis, reframing and rewriting of the material in conformity with Nature's formatting and reporting standards, and is not under simultaneous consideration at any other journal.

Authorship and contributorship

All listed authors meet the four ICMJE criteria for authorship: substantial contribution to conception or design, or to acquisition, analysis or interpretation of data; drafting or critical revision of the manuscript; final approval of the published version; and agreement to be accountable for all aspects of the work. No ghost-, gift- or guest-authorship occurred. No paid medical writers contributed to the manuscript.

Use of artificial intelligence (AI / LLM)

In accordance with Nature's policy on generative artificial intelligence (Nature 613:612, 2023), the authors disclose the following use of AI tools during the preparation of this manuscript:

- Large language model (LLM)-based writing assistants and the Microsoft Word grammar/style checker were used for language editing of the English manuscript translated from the original Ukrainian and Russian drafts, and to improve sentence-level clarity and concision.

- AI tools were also used to assist with formatting the document to Nature's author guidelines (sectioning, reference style, table layout, line and page numbering) and to assist with rendering of the graphical abstract layout.
- No AI tool was used to generate, design, simulate, fabricate or alter experimental data, to formulate the scientific hypothesis, to perform any of the histological or histochemical scoring, to select statistical methods or to produce the data figures (Figures 1 and 2).
- All scientific content, data, statistical claims, conclusions and references were generated, verified and approved by the human authors, who take full responsibility for the integrity and accuracy of the work.
- No LLM is listed as an author. Authorship implies accountability that current AI tools cannot bear.

Reporting standards

This work follows the ARRIVE 2.0 guidelines for reporting in vivo experiments (animals, sample size, allocation, blinding, end points, statistical methods). Subpopulation fractions are reported as group means; group sizes (n = 15) were predetermined and not adjusted post hoc. No animals were excluded after surgery; allocation to time-point subgroups was random; the experimenter performing the histological and histochemical scoring was blinded to group identity.

Additional information

Correspondence and requests for materials should be addressed to W. Zukow (zukow@umk.pl).

References

1. Gozhenko, A. I. Theory of disease: current state and topical problems. *J. Natl Acad. Med. Sci. Ukr.* **18**, 411–417 (2012).

2. Gozhenko, A. I. & Gryshko, Y. M. *Functional-Metabolic Continuum: Physiology and Pathology* (Ukrpromtorgservis, Poltava, 2020).

3. Rangel, A. O. The system: theory of living systems and relevance to CAM. Part II: theory. *Evid. Based Complement. Alternat. Med.* **2**, 129–137 (2005). https://doi.org/10.1093/ecam/neh068

4. Bowen, I. D. & Lockshin, R. A. (eds) *Cell Death in Biology and Pathology* (Chapman & Hall, London, 1981).

5. Strukov, A. I. *Pathological Anatomy* (Meditsina, Moscow, 1971).

6. Belushkina, N. N. & Severin, S. E. Molecular bases of apoptosis pathology. *Arkh. Patol.* **63**, 51–60 (2001).

7. Steller, H. Mechanisms and genes of cellular suicide. *Science* **267**, 1445–1449 (1995). https://doi.org/10.1126/science.7878463

8. Wyllie, A. H., Kerr, J. F. & Currie, A. R. Cell death: the significance of apoptosis. *Int. Rev. Cytol.* **68**, 251–306 (1980). https://doi.org/10.1016/s0074-7696(08)62312-8

9. Nasibullin, B. A. Structural and biochemical activity of thalamic structures of the brain. *Neurosci. Behav. Physiol.* **26**, 247–253 (1996).

10. Lovallo, W. R. & Gerin, W. Psychophysiological reactivity: mechanisms and pathways to cardiovascular disease. *Psychosom. Med.* **65**, 36–45 (2003). https://doi.org/10.1097/01.psy.0000033128.44101.c1

11. Gozhenko, A. I. *Foundations of the Theory of Disease* (Feniks, Odesa, 2015).

12. Iadecola, C. The pathobiology of vascular dementia. *Neuron* **80**, 844–866 (2013). https://doi.org/10.1016/j.neuron.2013.10.008

13. Lojda, Z., Gossrau, R. & Schiebler, T. H. *Enzyme Histochemistry: A Laboratory Manual* (Springer, Berlin, 1979).

14. Nasibullin, B. A. & Gozhenko, A. I. On the structural-functional correlates of homeostatic stability of the sensorimotor cortex in rats. *Patologiya* **1**, 47–59 (2004).

15. Nasibullin, B. A., Rozanov, V. A. & Yanovsky, M. B. Probabilistic analysis of the contribution of various metabolic pathways to neuronal bioenergetics in the main links of the vestibular analyser. *Neurokhimiya* **10**, 37–43 (1991).

16. European Parliament and Council. Directive 2010/63/EU on the protection of animals used for scientific purposes. *Off. J. Eur. Union* **L 276**, 33–79 (2010). http://data.europa.eu/eli/dir/2010/63/oj

17. Ministry of Education and Science, Youth and Sports of Ukraine. Order No. 249 of 1 March 2012 on the procedure for conducting experiments and experimental studies using laboratory animals. *Off. Bull. Ukr.* **24**, 82 (2012).

18. Nasibullin, B. A. Semi-quantitative scoring of dehydrogenase activity in cryostat sections of rat brain. *Neurokhimiya* **8**, 121–128 (1989).

19. Nature. Tools such as ChatGPT threaten transparent science; here are our ground rules for their use. *Nature* **613**, 612 (2023). https://doi.org/10.1038/d41586-023-00191-1